Science Advances
AAAS

advances.sciencemag.org/cgi/content/full/6/39/eabb6658/DC1

Supplementary Materials for

Achieving room-temperature brittle-to-ductile transition in ultrafine layered Fe-Al alloys

Lu-Lu Li, Yanqing Su, Irene J. Beyerlein*, Wei-Zhong Han*

*Corresponding author. Email: wzhanxjtu@mail.xjtu.edu.cn (W.-Z.H.); beyerlein@ucsb.edu (I.J.B.)

Published 23 September 2020, *Sci. Adv.* **6**, eabb6658 (2020)
DOI: 10.1126/sciadv.abb6658

This PDF file includes:

DFT Simulation methods

FeAl. To calculate the lattice parameter a_0, a simulation cell of B2-ordered FeAl, which contains one Fe atom and one Al atom, is used. The simulation cell size is varied, with the free energy calculated for each size. The lattice parameter a_0 corresponds to the cell size with the lowest free energy. The *k*-point mesh in these calculations is 11×11×11. It is found that a_0 = 2.874 Å at 0 K, which is close to the values reported from a prior DFT calculation at 0 K (2.895 Å) (*46*) and experiment at room temperature (2.969 Å) (*35*).

Two methods are used to calculate the GSFE curves: the standard one, which we refer to as unrelaxed and a more accurate one, called relaxed. To calculate the unrelaxed [111]($1\bar{1}0$) generalized stacking fault energies (GSFEs) γ_{gsf}, a unit cell containing 36 Fe atoms and 36 Al atoms is constructed. The crystallographic orientations are *x*[$1\bar{1}0$], *y*[$11\bar{2}$], and *z*[111]. Along the *x* direction, there are 24 atomic layers, each of which contains 3 atoms. A 12 Å vacuum is added to one end of the simulation cell along the *x* direction. For the GSFE calculations, a 1×15×15 *k*-point mesh is adopted. Along the *x* direction, the top 12 layers of atoms are displaced with respect to the bottom 12 atomic layers incrementally along the *z* direction, until the displacement d_z in the *z*-direction reaches $\sqrt{3}a_0$. In this way, the unrelaxed GSFE curve from one lattice point (a degenerate minimum) to the next one is generated by the energies associated with 41 distinct displacements. To calculate the relaxed GSFEs, following each displacement, the top two and bottom two layers of atoms are fixed, while the remaining atoms are allowed to relax along the *x* direction (*37*). The ionic relaxation stops when the total energy between two steps is smaller than 10^{-3} eV/atom.

The calculated unrelaxed GSFEs presented in Fig. 6A are compared against prior DFT calculations of B2-ordered FeAl (*46*,*47*). In these prior works, the unrelaxed method was used and the unrelaxed results computed here agree well with one of them (*46*). The relaxed GSFE curve shown in Fig. 6A, however, has not been reported previously.

$FeAl_2$. In $FeAl_2$, slip was seen to be localized on an unusually large number of distinct slip planes, with no obvious preferred slip mode. The crystal structure of $FeAl_2$ is triclinic and has a rather complex atomic configuration. Consequently, DFT calculations for the generalized stacking fault surfaces are too computationally intensive to repeat for all the observed slip planes. Unlike in FeAl, the <111>{110} slip system is not preferred in $FeAl_2$ until the bilayer thickness *t* reduces to the

submicron regime, when the phases co-deform and room temperature ductile behavior is achieved. Here we calculate using the same DFT method, the GSFE curves for the [111]($1\bar{1}0$) slip mode. For this slip system, a unit cell containing 48 Al atoms and 28 Fe atoms is used. The lattice parameters of $FeAl_2$ are taken from the experiment of Chumak et al. (*34*). As before, both the unrelaxed and relaxed curves are calculated.

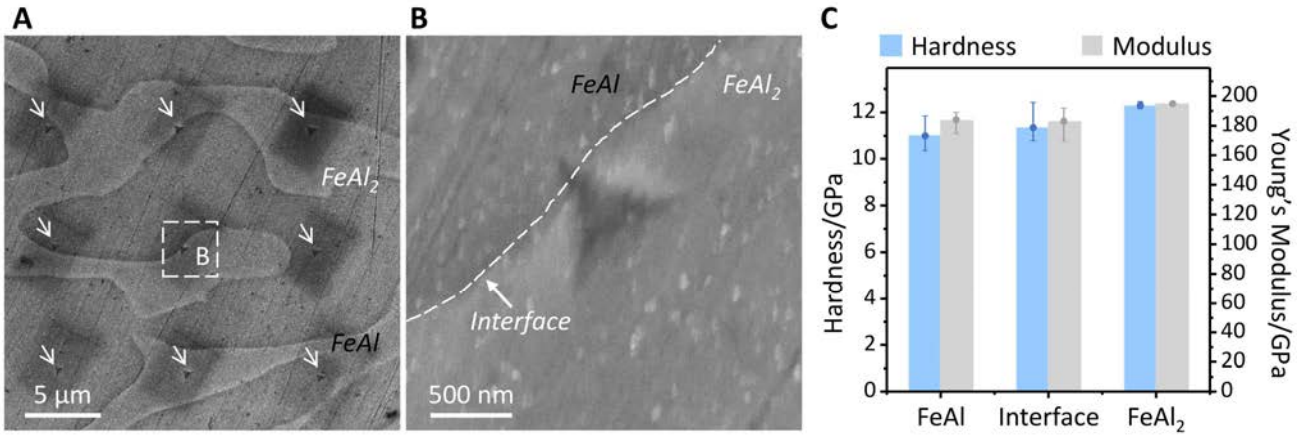

Fig. S1. Nano-indentation of layered FeAl/$FeAl_2$. (**A-B**) Typical SEM micrographs of indentations at the interface region of layered FeAl/$FeAl_2$. (**C**) The hardness and Young's modulus of single FeAl, $FeAl_2$ phases and at the interface region.

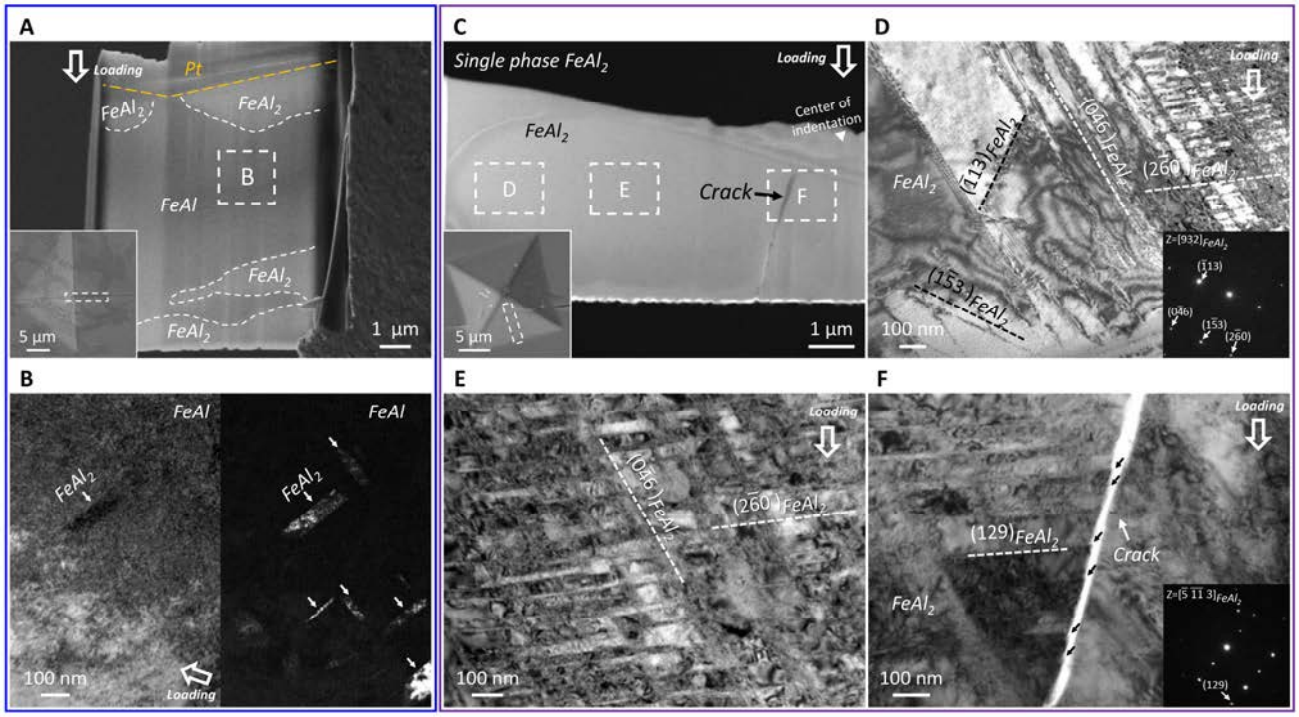

Fig. S2. Deformation of single phase FeAl and $FeAl_2$. (**A**) SEM micrograph of a lift-out sample from an indentation region with mixed FeAl and $FeAl_2$. (**B**) Deformation microstructures around the indentation in FeAl. (**C**) SEM micrograph of a lift-out sample from the indentation of $FeAl_2$ single phase. (**D-F**) Typical TEM images showing deformation microstructures around the indentation and a crack in single-phase $FeAl_2$.

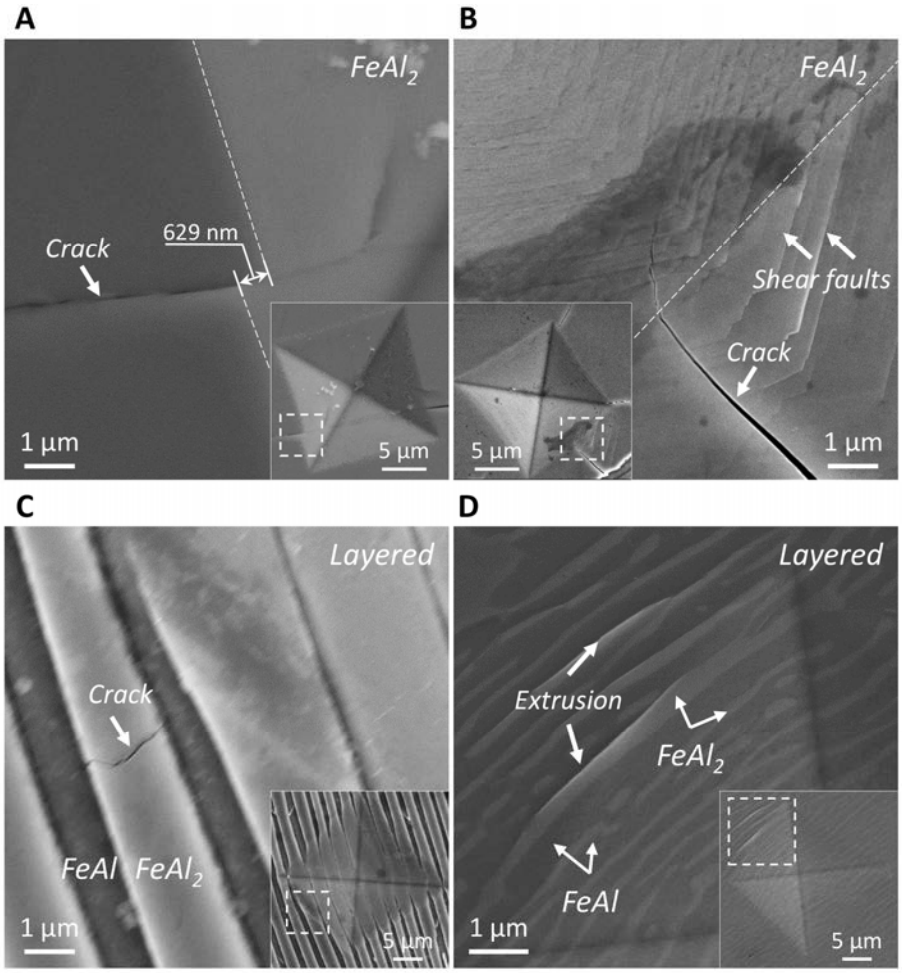

Fig. S3. Typical SEM micrographs displaying important deformation features produced around indentations in (**A** and **B**) single-phase $FeAl_2$, (**C** and **D**) the layered FeAl/$FeAl_2$. Major cracks have formed in single-phase $FeAl_2$ after indentation, while in the layered FeAl/$FeAl_2$, only a very small crack has formed in the $FeAl_2$ phase, which was blocked from propagating across the material by the ductile FeAl phase. Extrusions have formed around the indentation in the layered FeAl/$FeAl_2$.

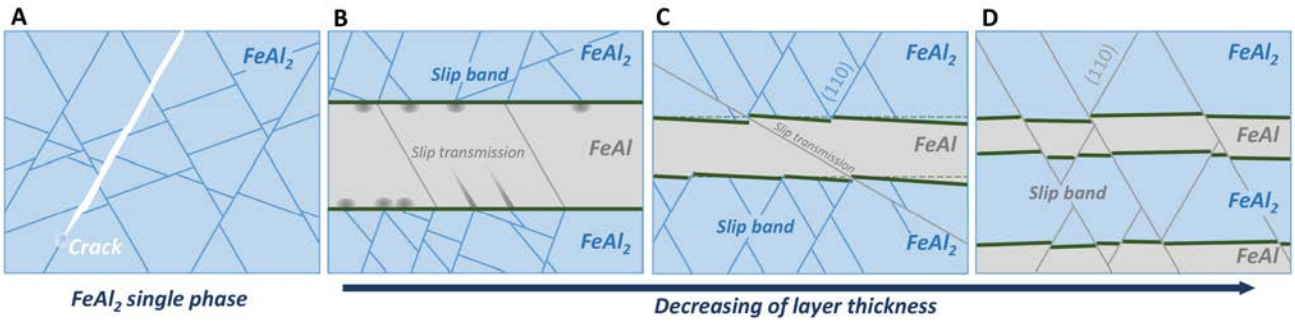

Fig. S4. Schematic showing the deformation mechanisms in Fe-Al alloy. (**A**) Slip localization and cracking in single phase $FeAl_2$. (**B-D**) Towards more homogeneous deformation with finer bilayer thickness, down into the submicron length scales in the Fe-Al alloy.